[Article] doi: 10.3866/PKU.WHXB201301211 www.whxb.pku.edu.cn

氧化石墨烯对水中内分泌干扰物双酚A的吸附性能

徐 婧[1] 朱永法[1,2,*]

([1]清华大学化学系, 北京 100084; [2]南京信息工程大学, 大气环境监测与污染控制高技术研究重点实验室, 南京 210044)

摘要: 以氧化石墨烯(GO)为吸附剂, 内分泌干扰物双酚A (BPA)为目标污染物, 考察了GO对水中BPA的吸附性能. 结果表明: GO对BPA的最大吸附量(q_m)约为87.80 mg·g^{-1} (25 °C), 30 min左右即可达到吸附平衡, 远快于活性碳; 吸附动力学和等温线数据分别符合准二级动力学模型和Langmuir吸附模型; 在溶液接近中性和低温的条件下有利于吸附的进行, 在溶液中存在电解质的条件下不利于吸附的进行. GO具有优异的循环吸附性能, 经过多次循环使用后依然可以保持良好的吸附能力. GO对BPA的吸附机理主要是由于GO本身的片状结构以及表面的含氧极性基团, 会与BPA之间产生$\pi-\pi$色散作用和氢键作用. 虽然GO对BPA的吸附能力不如石墨烯, 但是相比于石墨烯, GO表面含有大量极性基团, 具有良好的亲水性, 且GO合成方法相对简单, 可批量生产用于工业污水处理. 因此, 在水处理领域, GO有能力成为新型高效的吸附剂.

关键词: 吸附; 氧化石墨烯; 双酚A; 内分泌干扰物; 水处理

中图分类号: O647

Elimination of Bisphenol A from Water *via* Graphene Oxide Adsorption

XU Jing[1] ZHU Yong-Fa[1,2,*]

([1]*Department of Chemistry, Tsinghua University, Beijing 100084, P. R. China*; [2]*Jiangsu Key Laboratory of Atmospheric Environment Monitoring and Pollution Control, Nanjing University of Information Science and Technology, Nanjing 210044, P. R. China*)

Abstract: The elimination of bisphenol A (BPA) from aqueous solution by adsorption on graphene oxide (GO) was investigated. The maximum adsorption capacity (q_m) of GO for BPA estimated from the Langmuir isotherm was 87.80 mg·g^{-1} at 25 °C. The required contact time to reach adsorption equilibrium was about 30 min, which was much shorter than that of activated carbon. The adsorption kinetics and isotherm data fitted well with the pseudo-second-order kinetic model and the Langmuir isotherm, respectively. Neutral pH and low solution temperature were favorable for adsorption, whereas the presence of NaCl in the solution was unfavorable. The GO had good recyclability and could be reused several times with a slight decline in adsorption ability. Both hydrogen bonding and $\pi-\pi$ interaction were thought to be responsible for the adsorption of BPA on GO. The excellent adsorption capacity and high adsorption rate of GO result from its sheet-like structure and the abundant oxygen-containing groups on its surface. Although q_m of GO for BPA is lower than that of graphene, GO has the benefits of large scale production, a hydrophilic surface with plenty of oxygen-containing groups, and good dispersion in water. Therefore, GO can be regarded as a good potential adsorbent for water treatment.

Received: October 31, 2012; Revised: January 18, 2013; Published on Web: January 21, 2013.

*Corresponding author. Email: zhuyf@tsinghua.edu.cn; Tel/Fax: +86-10-62787601.

The project was supported by the National Key Basic Research Program of China (973) (2013CB632403), National High Technology Research and Development Program of China (863) (2012AA062701), Special Project on Innovative Method from the Ministry of Science and Technology of China (2009IM030500), and Atmospheric Environment Monitoring & Pollution Control Program of Jiangsu Province, China (AEMPC201103).
国家重点基础研究发展计划(973) (2013CB632403), 国家高技术研究发展计划(863) (2012AA062701), 科技部创新方法工作专项(2009IM030500)及江苏省大气环境监测与污染控制高技术研究重点实验室开放基金(AEMPC201103)资助项目

Key Words: Adsorption; Graphene oxide; Bisphenol A; Endocrine-disrupting chemical; Water treatment

1 Introduction

The European Commission has defined an endocrine-disrupting chemical (EDC) as "an exogenous substance that causes adverse health effects in an intact organism, or its progeny, consequent to changes in endocrine function".[1] EDCs can cause abnormalities in the functions of endocrine systems of wildlife and humans.[2] Therefore, EDCs have attracted increasing scientific and social attention in recent years. Bisphenol A (BPA), one of these EDCs, is widely used as an intermediate in the production of polycarbonates, epoxy resins, and other plastics. It is considered to be one kind of carcinogens and critical pollutants because it is harmful to organisms.[3,4] Although BPA is degradable under natural aerobic condition, it has been reportedly detected in wastewater, surface water, groundwater, and even drinking water.[5,6] Accordingly, BPA is extensively studied as the model compound for the removal from water among the phenolic EDCs.

It is important to develop advanced methods to remove BPA from aqueous solutions. Conventional methods are adsorption,[7−10] biological treatments,[11] photocatalytic degradation,[12] and other processes, among which adsorption has been found to be a superior and rapid removal method as it is low cost, easy to operate, and no secondary pollutants. Regarding the adsorption technique, an effective adsorbent is crucial to guaranteeing the efficiency of water treatment. Common adsorbent materials include activated carbon (AC),[13] carbon nanomaterials,[7,14] carbon nanotubes,[15] graphene,[16,17] silicas,[10] etc.[9,18,19] Among them, AC has been the most commonly used for the removal of organic contaminants.[20] Nevertheless, considering its low absorption rate, high content of impurities, difficulty of circulating operation, AC is not perfect enough to meet the need of industrial usages. Therefore, it is still necessary to develop new effective adsorbent materials with a high adsorption capacity, good stability, and fast adsorption rate.

Graphite oxide (GO), an oxygen-rich derivative of graphite, has been extensively investigated in recent years. It exhibits an extended layered structure with plenty of hydrophilic oxygen-containing groups (— OH, — COOH, — CHO, and epoxy groups) on the graphitic backbone.[21,22] Additionally, GO can be obtained from cheap natural graphite in large quantities, and shows excellent adsorption capacity for the removal of heavy metal ions,[23−25] dyes,[26,27] and antibiotics[28] from aqueous solutions. However, no reports regarding the application of GO on BPA removal has been reported to the best of our knowledge.

In this paper, the removal behavior of BPA from water by GO as a function of solution characteristics, including BPA concentration, pH, ionic strength, and temperature, was investigated systematically. The adsorption capacity was evaluated and adsorption mechanism of BPA by GO was proposed.

2 Materials and methods

2.1 Synthesis of GO

All chemicals used were analytic grade reagents without further purification. GO was synthesized by a modified Hummers method.[29,30] Graphite (2.0 g) and $NaNO_3$ (1.0 g) were mixed with 50 mL of H_2SO_4 (98% (*w*)) in a 500 mL flask and stirred for 30 min in an ice bath. Then $KMnO_4$ (6.0 g) was dropped into the vigorously stirred suspension below 15 °C. The ice bath was then removed, and the mixture was stirred at room temperature until it gradually became a brownish slurry, and then diluted slowly with 100 mL of water. The reaction temperature was rapidly increased to 98 °C with effervescence and the colour of suspension changed to brown. After that, 200 mL of water and 10 mL of H_2O_2 (30% (*w*)) were successively added. For purification, the mixture was centrifuged and washed with 10% HCl and then deionized water several times to remove the residual metal ions and acid. After filtration and drying under vacuum at room temperature, GO was obtained as powder.

2.2 Characterization

The samples were characterized by powder X-ray diffraction (XRD) on a Bruker D8-advance X-ray diffractometer at 40 kV and 40 mA for monochromatized Cu K_α (λ=0.1541 nm) radiation. The Brunauer-Emmett-Teller (BET) specific surface area of the samples was characterized by nitrogen adsorption at 77 K with a Micromeritics 3020 instrument. Zeta potential measurements were made with a Delsa Nano C zeta potential instrument (Beckman Coulter). Atomic force microscope (AFM) images were acquired in phase mode in air using Digital Instruments Shimadzu SPM-9600 (The samples were prepared by drop-casting corresponding dilute dispersions onto a freshly cleaved mica surface). Fourier transform infrared (FTIR) spectra were recorded on a Thermo Nicolet Avatar 370 spectrometer between 4000 and 400 cm^{-1} using KBr pellets.

2.3 Batch adsorption experiments

BPA ($(CH_3)_2C(C_6H_4OH)_2$, molecular weight 228.29) was purchased from the Beijing Chemical Works, China. It is a hydrophobic compound with a low solubility in water. BPA is in the molecular form at pH<8.0 and starts the first deprotonation at around pH 8.0 and the second one at around pH 9.0. It is mostly ionized to monovalent or divalent anions after the deprotonation.[13] BPA possesses hydroxyl groups which can generate hydrogen bonding with adsorbents. Herein, BPA was dissolved in ethanol as a stock solution (1000 $mg \cdot L^{-1}$) and was further diluted with a large amount of water to the required concentrations before used.

All adsorption experiments were performed in sealed 250 mL glass conical bottles in a shaking water bath at a shaking speed of 200 $r \cdot min^{-1}$ at the appropriate temperature. Every bottle contained 10 mg of GO and 100 mL of BPA solution in the

appropriate concentration.

An adsorption kinetic study was obtained with an initial BPA concentration of 10 mg·L^{-1} at 25 °C, pH 6.0 to determine the time required for adsorption to reach equilibrium. The concentrations of BPA were measured at different time intervals from 5 to 300 min.

Adsorption isotherm of BPA on GO was carried out at 25 °C, pH 6.0, with different initial BPA concentrations ranging from 2 to 50 mg·L^{-1}.

The effect of pH on the adsorption of BPA was examined with an initial BPA concentration of 10 mg·L^{-1} in a pH range of 2.0–11.0 at 25 °C. The solution pH was regulated by adding 0.1 mol·L^{-1} HCl or NaOH solution.

The effect of the ionic strength on the adsorption of BPA was examined by adding NaCl to 10 mg·L^{-1} BPA solutions with concentrations ranging from 0.02 to 0.5 mol·L^{-1} at 25 °C, pH 6.0.

The effect of the temperature on the adsorption of BPA was examined with an initial BPA concentration of 10 mg·L^{-1} at pH 6.0 at different temperatures of 15, 25, 35, and 45 °C, respectively.

After adsorption experiments, the suspensions were centrifuged at 12000 r·min^{-1} for 10 min, and the supernatant was filtered through 0.45 μm membrane. The concentration of BPA was examined by a high-performance liquid chromatography (HPLC, Lumtech) system with a Venusil XBP-C18 column (Agela Technologies Inc.) and using a UV absorbance detector (K2501) operated at 280 nm. The mobile phase was 1.0 mL·min^{-1} of 70% methanol and 30% deionized water.

3 Results and discussion

3.1 Properties of graphene oxide

XRD patterns for graphite and GO were obtained and shown in Fig.S1 (Supporting Information). Graphite exhibited a very sharp (002) diffraction peak at 26.4°. The 2θ value corresponded to an interlayer spacing of about 0.34 nm. Oxidation treatment caused a decrease in the (002) peak intensity of graphite, and a (001) diffraction peak of GO appeared at 11.0°. This (001) peak demonstrated the typical loose-layer-like structure due to the intercalating oxygen-containing groups. The corresponding interlayer spacing of GO was about 0.80 nm which was evidently larger than that of graphite. The interlayer spacing might be dependent on the preparing method and the amount of water remained in the gallery space of GO.[24]

N_2 adsorption-desorption isotherms for graphite and GO were determined in Fig.S2a (Supporting Information). Graphite and GO both showed the type IV isotherms classified by IUPAC with hysteresis loops observed in the relative pressure (p/p_0) range of 0.45–1.00, suggesting the mesoporous property.[31] Owing to the severe aggregation of GO sheets during desiccation, GO exhibited a relatively low BET specific surface area of 32 m^2·g^{-1}, which was still higher than that of graphite (15.9 m^2·g^{-1}). The pore size distribution of GO was more remarkable than that of graphite (Fig.S2b (Supporting Information)). The width of the pores in GO sheets was mainly 3.6 nm. Since the largest length of BPA molecule was 0.94 nm,[13] the pore size of GO was big enough for BPA molecules to access to the functional groups on the surface of mesostructures. Thus, GO could be a good candidate as adsorbent.

The stability of GO dispersions was examined by the zeta potential analysis. The zeta potentials of GO dispersions were always negative throughout the whole pH range, which indicated the presence of negative charges on the surface of the GO sheets (Fig.S3 (Supporting Information)). The zeta potentials were below −30 mV for pH>5.0 and can reach −40 mV for pH 10.0. Zeta potentials lower than −30 mV generally imply sufficient mutual repulsion which can ensure the stability of a dispersion, as well known in colloidal science.[33] Therefore, the excellent stability of GO dispersions was mainly attributed to the electrostatic repulsion among the GO sheets.

The morphological structure of GO was characterized by AFM. The AFM image (Fig.S4a (Supporting Information)) showed that the GO sheets were almost transparent with a flake-like shape. The partial overlap of the GO sheets caused different brightness values on the surface of GO. The sizes of the GO sheets were ranging from several tens of nanometers to several micrometers. The cross-section analysis of GO (Fig. S4b (Supporting Information)) indicated that the average height of the GO sheets was about 1.0 nm which meant that GO existed mainly in a single-layer state in aqueous solution. Similar results had also been reported in other AFM studies of GO.[23,34]

3.2 BPA adsorption kinetics

Adsorption kinetics was investigated for a better understanding of the dynamics of adsorption. The concentration of BPA in aqueous solution without GO did not change after 300 min (Fig.S5 (Supporting Information)). This blank experiment indicated that BPA cannot be decomposed by itself. The effect of contact time on the adsorption of BPA by GO was shown in Fig.1. The adsorption achieved equilibrium in a short time of about 30 min, suggested that GO showed very rapid adsorption

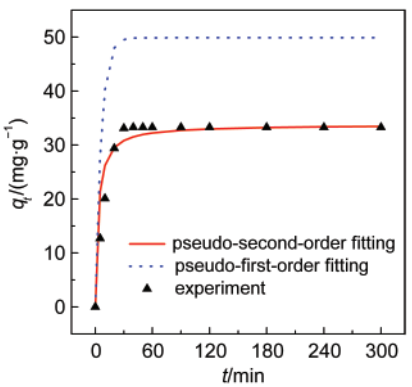

Fig.1 Effect of contact time on the adsorption of BPA by GO
condition: 10 mg of GO and 100 mL of BPA (10 mg·L^{-1}) reacted at 25 °C, pH 6.0. q_t: the amount of BPA adsorbed on GO at various time

Table 1 Kinetic parameters for the adsorption of BPA by GO

$q_{e,exp}$/(mg·g^{-1})	Pseudo-first-order			Pseudo-second-order			
	k_1/min^{-1}	$q_{e,cal}$/(mg·g^{-1})	R^2	k_2/(g·mg^{-1}·min^{-1})	$q_{e,cal}$/(mg·g^{-1})	h/(mg·g^{-1}·min^{-1})	R^2
33.30	0.16	49.88	0.908	0.010	33.80	11.63	0.999

rate and high industrial application value. On the basis of the above result, the contact time of 2 h was selected for a sure establishment of the adsorption equilibrium in further adsorption studies.

The adsorption capacity of GO for BPA was calculated according to the following equation:

$$q_e=(C_0-C_e)V/m \quad (1)$$

where C_0 and C_e represent the initial and equilibrium concentrations of BPA aqueous solution (mg·L^{-1}), V is the volume of the solution (L), and m is the mass of the adsorbent (g).

To investigate the adsorption kinetics of BPA by GO, two conventional kinetic models (pseudo-first-order and pseudo-second-order) were adopted to simulate the experimental data.

The pseudo-first-order model can be expressed as[35]

$$\ln(q_e-q_t)=\ln q_e-k_1t \quad (2)$$

where q_e and q_t are the amounts of BPA adsorbed on GO at equilibrium and at various time t (mg·g^{-1}), respectively, and k_1 is the rate constant of the pseudo-first-order model of adsorption (min^{-1}). The values of q_e and k_1 can be determined from the intercept and slope of the linear plot of $\ln(q_e-q_t)$ *versus* t.

The pseudo-second-order model includes all the steps of adsorption including external film diffusion, adsorption, and internal particle diffusion, which is described as[36,37]

$$t/q_t=1/k_2q_e^2+t/q_e \quad (3)$$

where q_e and q_t are defined as in the pseudo-first-order model and k_2 is the rate constant of the pseudo-second-order model for adsorption (g·mg^{-1}·min^{-1}). The slope and intercept of the linear plot of t/q_t against t yield the values of q_e and k_2. Furthermore, the initial adsorption rate h (mg·g^{-1}·min^{-1}) can be determined from $h=k_2q_e^2$.

Table 1 presented the kinetic parameters for the removal of BPA by GO. The correlation coefficient R^2 value for the pseudo-second-order model exceeded 0.99, which was much higher than that of the pseudo-first-order model. Moreover, the calculated adsorption capacity ($q_{e,cal}$) obtained from the pseudo-second-order model also coincided well with the experimental adsorption capacity ($q_{e,exp}$). These results indicated that the pseudo-second-order kinetic model provided a better correlation in contrast to the pseudo-first-order model for the adsorption of BPA on GO.

3.3 BPA adsorption isotherms

The adsorption isotherm models are usually used to fit experiment data and help to explore the adsorption mechanism more deeply. It can be seen in Fig.2 that the adsorption capacity of GO increased with the increasing equilibrium concentration of BPA and reached saturation progressively, as the increase in BPA concentration could accelerate the diffusion of BPA molecules onto the GO sheets. The Langmuir and the Freundlich isotherms are the most frequently used models to describe the equilibrium data of adsorption from aqueous solution.

The Langmuir isotherm assumes monolayer coverage of the adsorption surface and no subsequent interaction among adsorbed molecules. The expression for the Langmuir isotherm is[38]

$$C_e/q_e=C_e/q_m+1/(q_mK_L) \quad (4)$$

where q_e is the adsorbed BPA amount per gram of GO (mg·g^{-1}), C_e represents the equilibrium concentration of BPA in solution (mg·L^{-1}), K_L is the Langmuir constant (L·mg^{-1}), which is related to the affinity of the binding sites, and q_m represents the maximum adsorption capacity of the adsorbents (mg·g^{-1}). The values of q_m and K_L are calculated from the slope and intercept of the linear plot of C_e/q_e against C_e.

The Freundlich isotherm is derived to model multilayer adsorption and adsorption on heterogeneous surfaces. It can be described as[39]

$$\ln q_e=(\ln C_e)/n+\ln K_F \quad (5)$$

where q_e and C_e are defined as in the Langmuir isotherm; K_F and n are the Freundlich constants that represent the adsorption capacity and the adsorption strength, respectively. The magnitude of $1/n$ quantifies the favourability of adsorption and the degree of heterogeneity of the surface of GO. If $n>1$, suggesting favourable adsorption, then the adsorption capacity increases and new adsorption sites form.[40] K_F and n can be obtained from the intercept and slope of the linear plot of $\ln q_e$ *versus* $\ln C_e$.

The isotherm parameters were calculated and listed in Table 2. On the basis of a comparison of the correlation coefficient R^2 values, the Langmuir model fit the adsorption data better than the Freundlich model. In other words, this adsorption process took place at the functional groups on the surface of GO sheets, which was regarded as monolayer adsorption. In addition, it can be calculated from the Langmuir equation that q_m was 87.80 mg·g^{-1}.

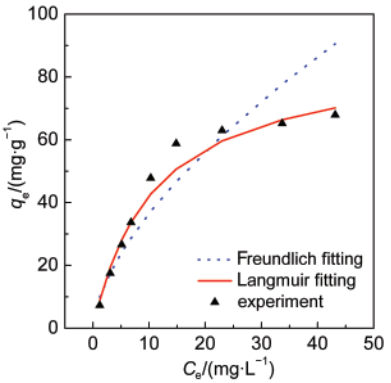

Fig.2 Adsorption isotherms of BPA by GO

condition: 10 mg of GO and 100 mL of BPA (10 mg·L^{-1}) reacted for 2 h at 25 °C, pH 6.0

Table 2 Isotherm parameters for the adsorption of BPA by GO

Langmuir			Freundlich		
q_m/(mg·g^{-1})	K_L/(L·mg^{-1})	R^2	K_F	n	R^2
87.80	0.0920	0.980	8.734	1.610	0.910

For comparison, the adsorption capacities of other common adsorbents in the literature were also summarized in Table S1. Compared with them, the adsorption capacity of GO was the highest. Considering the BET surface area of the adsorbents, the high affinity of GO to BPA was even more obvious. Besides, the adsorption rate of GO had also been compared with that of AC.[10] The required contact time to reach equilibrium was approximately 30 and 120 min for GO and AC, respectively. This implied that the attachment of BPA to the surface of GO was faster than that of AC. These results indicated that GO was an excellent BPA absorbent with high capacity and rate.

3.4 Effect of the solution pH, ionic strength and temperature

The solution pH is one of the most important parameters affecting the adsorption process in aqueous solution.[41] Fig.3(a) showed the effect of the solution pH on BPA adsorption by GO, with the initial pH ranging from 2.0 to 11.0. With the increasing pH, the adsorption capacity of GO firstly increased and then decreased, the maximum was at pH 6.0. These phenomena can be explained by the net charge of GO and BPA at different pH values. GO was negatively charged over the whole pH range, which was shown by the zeta potential analysis (Fig.S3). BPA was in its molecular form at pH<8.0 and started the first deprotonation at around pH 8.0 and the second at around pH 9.0. It was mostly ionized to monovalent or divalent anions after the deprotonation.[13] Therefore, the increase in adsorption capacity of GO in the acidic pH range might be due to the competition between hydrogen ions and BPA for the adsorption sites on GO. With increasing the pH value, there were fewer hydrogen ions in solution, which led to more binding sites available for BPA. The reduction in the adsorption capacity of GO observed in the alkaline pH range was partly owing to the repulsive electrostatic interactions established between the negatively charged GO surface and the bisphenolate anion.

It is well known that industrial sewage contains not only pollutants but also high concentrations of salts, which may affect the removal of pollutants. Thus, a study was also conducted on the effect of the solution ionic strength on the adsorption of BPA by GO. We can see that the adsorption capacity of GO was decreased in the presence of NaCl in solution (Fig.3(b)). This indicated that NaCl was more competitive than BPA for adsorption sites on GO. The binding sites of GO available for BPA were occupied by NaCl. However, the adsorption capacity was increased slightly when the NaCl concentration exceeded 0.1 mol·L^{-1}. This phenomenon can be attributed to the salting-out effect of electrolytes *via* decreasing the solubility of BPA and enhancing its adsorption on GO.[8,13]

The effect of the solution temperature on the adsorption of BPA by GO was also investigated under four different temperatures (Fig.3(c)). With increasing the temperature, the decline in the adsorption capacity of GO was observed. It indicated that the adsorption of BPA on GO was unfavorable at higher temperature and the adsorption reaction was an exothermic process.[8]

3.5 Regeneration study of GO

The recyclability of GO was determined by investigating the adsorption ability of the regenerated GO. In this part, 10 mg of GO was first mixed with 100 mL of BPA solution (10 mg·L^{-1}) for 2 h at 25 °C, pH 6.0. Then the above BPA adsorbed GO was dispersed in an aqueous solution (100 mL) containing ethanol (10% (volume fraction)) for elution. The desorption efficiency (η) can be determined from the following equation:

$$\eta = C_t V / q_e m \times 100\% \quad (6)$$

where C_t represents the concentration of BPA aqueous solution at a given time (mg·L^{-1}), q_e is the amount of BPA adsorbed on GO at equilibrium (mg·g^{-1}), V is the volume of the solution (L), and m is the mass of the adsorbent (g).

After BPA was completely desorbed from GO, it was thoroughly washed with water, filtered and dried in a vacuum. The regenerated GO was then applied to the repeated adsorption/desorption cycles to study the recyclability of GO.

The desorption efficiency was shown in Fig.4(a). It can be seen that BPA gradually desorbed from GO. After 300 min, about 91% of BPA adsorbed on GO previously had desorbed into the solution. From Fig.4(b), it was found that the adsorp-

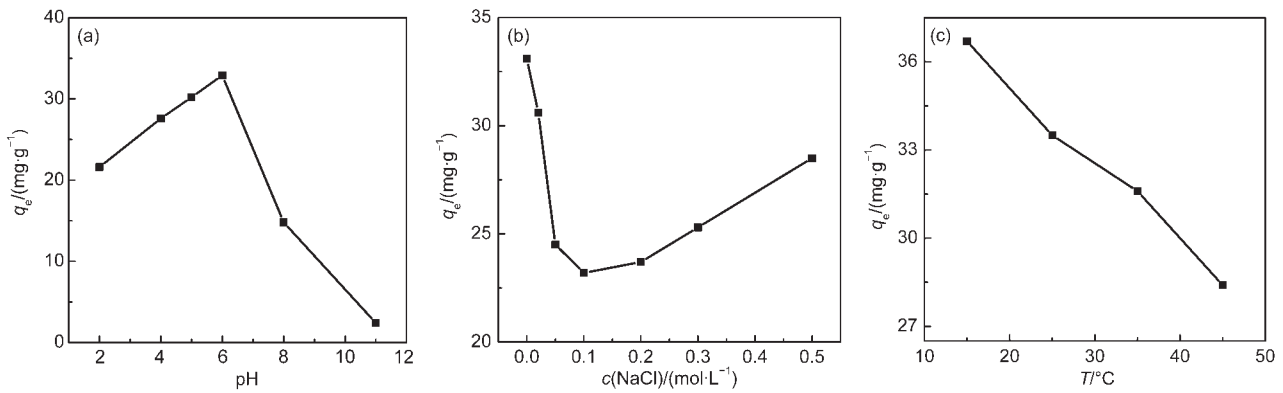

Fig.3 Effects of the solution pH (a), ionic strength (b), and temperature (c) on the adsorption of BPA by GO

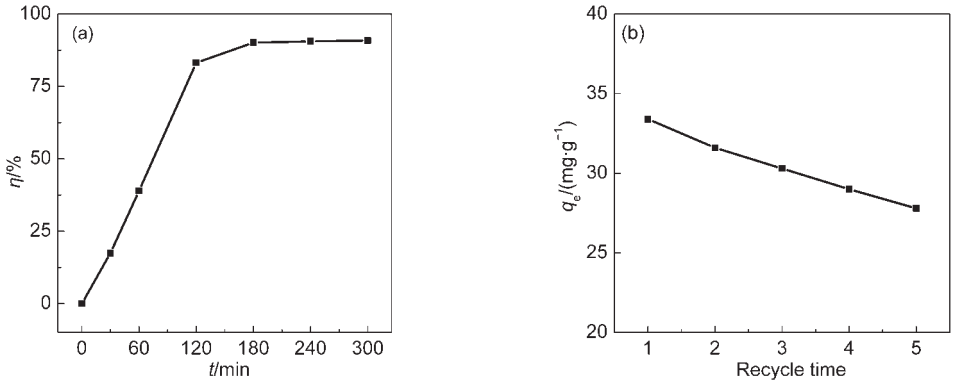

Fig.4 (a) Desorption efficiency (η) of GO and (b) re-adsorption of GO

condition: 10 mg of GO and 100 mL of BPA (10 mg·L^{-1}) reacted for 2 h at 25 °C, pH 6.0

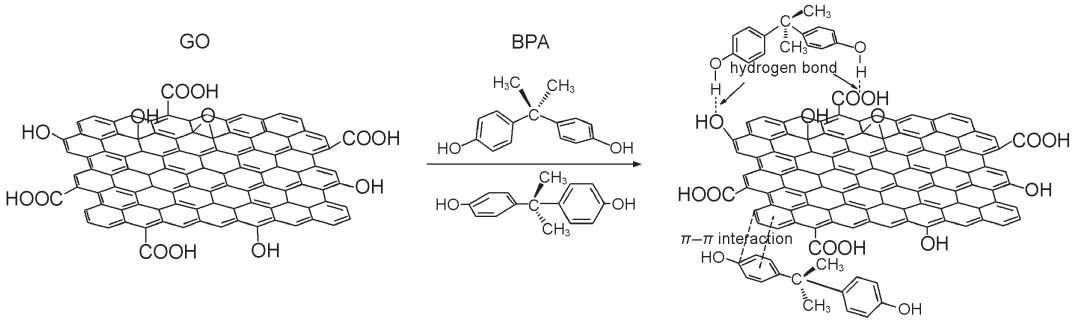

Fig.5 Schematic of hydrogen bonding and π–π interaction between GO and BPA

tion capacity of GO for BPA declined from 33.3 to 27.8 mg·g^{-1} after five time cycles. Compared with the first adsorption, the fifth one decreased by about 17% which still indicated the good reusability of GO. Thus, due to its excellent recyclability, GO is qualified for practical application.

3.6 Adsorption mechanism

GO contained hydrophobic graphene basal planes with aromatic rings and hydrophilic groups such as hydroxyl (—OH) and carboxyl (O=C—O). BPA also had both hydrophobic phenyl groups and hydrophilic hydroxyl groups. Due to the similar composition of BPA and GO, it was expected that two kinds of adsorbent–adsorbate interactions might be responsible for the adsorption of BPA on GO.[10] One possible interaction was hydrogen bonding between the hydrophilic groups of GO and BPA. The other was π–π interaction between the benzene rings contained in both BPA and GO.[42] Fig.5 showed the schematic of hydrogen bonding and π–π interaction between BPA and GO. The interactions between BPA and GO were also investigated using the FTIR spectra of GO and GO after BPA adsorption.

FTIR spectroscopy has been used as a useful tool in identifying the presence of certain functional groups on the surface of a solid. In Fig.6, the FTIR spectrum of GO showed broad absorption at 3418 cm^{-1}, which corresponded to —OH groups. The peak at 1727 cm^{-1} indicated the existence of C=O bonds in carboxylic acid and carbonyl moieties. The peak at 1622 cm^{-1} may be from skeletal vibrations of aromatic C=C bonds. The peak around 1383 cm^{-1} belonged to carboxyl O=C—O bonds. The peak at 1223 cm^{-1} was from epoxy C—O—C bonds. The peak around 1048 cm^{-1} referred to alkoxy C—O bonds.[43] The FTIR spectrum of GO after BPA adsorption displayed that the stretching frequency of hydroxyl groups shifted from 3418 to 3433 cm^{-1}. This indicated that there might be hydrogen bonding between hydroxyl groups of BPA and hydrophilic groups of GO.[10] The band corresponding to aromatic groups at 1622 cm^{-1} broadened obviously compared to that of GO. This proved that there might be π–π interaction between the phenyl groups of BPA and the graphene planes with linked aromatic rings of GO.[44] Therefore, the result of the FTIR spectroscopy was a new evidence in proving the presence of hydrogen bonding and π–π interaction between GO and BPA.

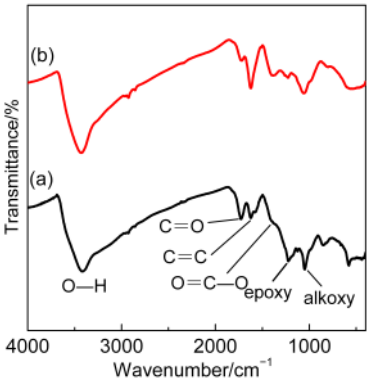

Fig.6 FTIR spectra of GO (a) and GO after BPA adsorption (b)

4 Conclusions

GO showed excellent adsorption capacity and high adsorption rate for BPA. The maximum adsorption capacity of GO for BPA estimated from the Langmuir isotherm was 87.80 mg·g^{-1} at 25 °C. Besides, the required contact time to reach the adsorption equilibrium was about 30 min. The effect of the experimental conditions on the adsorption properties of GO in aqueous solution has been demonstrated. The kinetics and isotherm data were fit well with the pseudo-second-order kinetic model and the Langmuir isotherm, respectively. The neutral pH and low temperature of the solution were favorable for the adsorption, whereas the presence of NaCl in the solution was unfavorable. GO has good recyclability, can retain about 83% of their adsorption ability after five adsorption-desorption cycles. The large adsorption affinity of GO for BPA seems to be attributed to its hydrophobic graphene planes with aromatic rings and hydrophilic oxygen-containing groups, which can generate $\pi-\pi$ interaction and hydrogen bonds with two benzene rings and two hydroxyl groups of BPA, respectively. The adsorption mechanism was also proved by the FTIR spectra of GO and GO after BPA adsorption. Although the adsorption capacity of GO for BPA is lower than that of graphene,[16] GO has its own available superiorities, like large quantity production, hydrophilic surface with plenty of oxygen-containing groups, and good dispersion in water. Therefore, GO is a potential adsorbent for water treatment.

Supporting Information: XRD patterns of graphite and GO (Fig.S1). Nitrogen adsorption-desorption isotherms and the pore size distribution of graphite and GO (Fig.S2). Zeta potential analysis of GO dispersion (Fig.S3). AFM image and cross-section analysis of GO (Fig.S4). The blank experiment of BPA concentration change without GO *versus* time (Fig.S5). Adsorption capacity of BPA by GO in comparison to other literature values (Table S1). This information is available free of charge *via* the internet at http://www.whxb.pku.edu.cn.

References

(1) Snyder, S. A.; Westerhoff, P.; Yoon, Y.; Sedlak, D. L. *Environ. Sci. Technol.* **2003,** *20*, 449.

(2) Chang, H. S.; Choo, K. H.; Lee, B.; Choi, S. J. *J. Hazard. Mater.* **2009,** *172*, 1. doi: 10.1016/j.jhazmat.2009.06.135

(3) Kang, J. H.; Kondo, F.; Katayama, Y. *Toxicology* **2006,** *226*, 79. doi: 10.1016/j.tox.2006.06.009

(4) Staples, C. A.; Dorn, P. B.; Klecka, G. M.; O′Block, S. T.; Harris, L. R. *Chemosphere* **1998,** *36*, 2149. doi: 10.1016/S0045-6535(97)10133-3

(5) Staples, C. A.; Dorn, P. B.; Klecka, G. M.; O′Block, S. T.; Branson, D. R.; Harris, L. R. *Chemosphere* **2000,** *40*, 521. doi: 10.1016/S0045-6535(99)00288-X

(6) Belfroid, A.; van Velzen, M.; van der Horst, B.; Vethaak, D. *Chemosphere* **2002,** *49*, 97. doi: 10.1016/S0045-6535(02)00157-1

(7) Pan, B.; Lin, D. H.; Mashayekhi, H.; Xing, B. S. *Environ. Sci. Technol.* **2009,** *43*, 5480.

(8) Liu, G. F.; Ma, J.; Li, X. C.; Qin, Q. D. *J. Hazard. Mater.* **2009,** *164*, 1275. doi: 10.1016/j.jhazmat.2008.09.038

(9) Dong, Y.; Wu, D. Y.; Chen, X. C.; Lin, Y. *J. Colloid Interface Sci.* **2010,** *348*, 585. doi: 10.1016/j.jcis.2010.04.074

(10) Kim, Y. H.; Lee, B.; Choo, K. H.; Choi, S. J. *Microporous Mesoporous Mat.* **2011,** *138*, 184. doi: 10.1016/j.micromeso.2010.09.007

(11) El-Naas, M. H.; Al-Muhtaseb, S. A.; Makhlouf, S. *J. Hazard. Mater.* **2009,** *164*, 720. doi: 10.1016/j.jhazmat.2008.08.059

(12) Wang, R.; Ren, D.; Xia, S.; Zhang, Y.; Zhao, J. *J. Hazard. Mater.* **2009,** *169*, 926. doi: 10.1016/j.jhazmat.2009.04.036

(13) Bautista-Toledo, I.; Ferro-Garcia, M. A.; Rivera-Utrilla, J.; Moreno-Castilla, C.; Vegas Fernandez, F. J. *Environ. Sci. Technol.* **2005,** *39*, 6246. doi: 10.1021/es0481169

(14) Pan, B.; Xing, B. S. *J. Agric. Food Chem.* **2010,** *58*, 8338. doi: 10.1021/jf101346e

(15) Kuo, C. Y. *Desalination* **2009,** *249*, 976. doi: 10.1016/j.desal.2009.06.058

(16) Xu, J.; Wang, L.; Zhu, Y. F. *Langmuir* **2012,** *28*, 8418. doi: 10.1021/la301476p

(17) Yuan, W. H.; Li, B. Q.; Li, L. *Acta Phys. -Chim. Sin.* **2011,** *27*, 2244. [袁文辉, 李保庆, 李 莉. 物理化学学报, **2011,** *27*, 2244.] doi: 10.3866/PKU.WHXB20110838

(18) Nakanishi, A.; Tamai, M.; Kawasaki, N.; Nakamura, T.; Tanada, S. *J. Colloid Interface Sci.* **2002,** *252*, 393. doi: 10.1006/jcis.2002.8387

(19) Asada, T.; Oikawa, K.; Kawata, K.; Ishihara, S.; Iyobe, T.; Yamada, A. *J. Health Sci.* **2004,** *50*, 588. doi: 10.1248/jhs.50.588

(20) Furhacker, M.; Scharf, S.; Weber, H. *Chemosphere* **2000,** *41*, 751. doi: 10.1016/S0045-6535(99)00466-X

(21) Dikin, D. A.; Stankovich, S.; Zimney, E. J.; Piner, R. D.; Dommett, G. H. B.; Evmenenko, G.; Nguyen, S. T.; Ruoff, R. S. *Nature* **2007,** *448*, 457. doi: 10.1038/nature06016

(22) Dreyer, D. R.; Park, S.; Bielawski, C. W.; Ruoff, R. S. *Chem. Soc. Rev.* **2010,** *39*, 228. doi: 10.1039/b917103g

(23) Yang, S. T.; Chang, Y. L.; Wang, H. F.; Liu, G. B.; Chen, S.; Wang, Y. W.; Liu, Y. F.; Cao, A. N. *J. Colloid Interface Sci.* **2010,** *351*, 122. doi: 10.1016/j.jcis.2010.07.042

(24) Zhang, K.; Dwivedi, V.; Chi, C. Y.; Wu, J. S. *J. Hazard. Mater.* **2010,** *182*, 162. doi: 10.1016/j.jhazmat.2010.06.010

(25) Nana, Z.; Haixia, Q.; Youmiao, S.; Wei, W.; Jianping, G. *Carbon* **2011,** *49*, 827. doi: 10.1016/j.carbon.2010.10.024

(26) Fan, L.; Luo, C.; Li, X.; Lu, F.; Qiu, H.; Sun, M. *J. Hazard. Mater.* **2012,** *215–216*, 272.

(27) Zhang, W.; Zhou, C.; Zhou, W.; Lei, A.; Zhang, Q.; Wan, Q.; Zou, B. *Bull. Environ. Contam. Toxicol.* **2011,** *87*, 86. doi: 10.1007/s00128-011-0304-1

(28) Gao, Y.; Li, Y.; Zhang, L.; Huang, H.; Hu, J.; Shah, S. M.; Su,

X. *J. Colloid Interface Sci.* **2012,** *368*, 540. doi: 10.1016/j.jcis.2011.11.015

(29) Hummers, W. S.; Offeman, R. E. *J. Am. Chem. Soc.* **1958,** *80*, 1339. doi: 10.1021/ja01539a017

(30) Hu, Y. J.; Jin, J.; Zhang, H.; Wu, P.; Cai, C. X. *Acta Phys. -Chim. Sin.* **2010,** *26*, 2073. [胡耀娟, 金 娟, 张 卉, 吴 萍, 蔡称心. 物理化学学报, **2010,** *26*, 2073.] doi: 10.3866/PKU.WHXB20100812

(31) Sing, K. S. W.; Everett, D. H.; Haul, R. A. W.; Moscou, L.; Pierotti, R. A.; Rouquerol, J.; Siemieniewska, T. *Pure Appl. Chem.* **1985,** *57*, 603. doi: 10.1351/pac198557040603

(32) Everett, D. H. *Basic Principles of Colloid Science*; The Royal Society of Chemistry: London, 1988.

(33) Fan, X. B.; Peng, W. C.; Li, Y.; Li, X. Y.; Wang, S. L.; Zhang, G. L.; Zhang, F. B. *Adv. Mater.* **2008,** *20*, 4490. doi: 10.1002/adma.v20:23

(34) Ho, Y. S.; McKay, G. *Water Res.* **2000,** *34*, 735. doi: 10.1016/S0043-1354(99)00232-8

(35) Blanchard, G.; Maunaye, M.; Martin, G. *Water Res.* **1984,** *18*, 1501. doi: 10.1016/0043-1354(84)90124-6

(36) Zhao, G. X.; Li, J. X.; Wang, X. K. *Chem. Eng. J.* **2011,** *173*, 185. doi: 10.1016/j.cej.2011.07.072

(37) Langmuir, I. *J. Am. Chem. Soc.* **1916,** *38*, 2221. doi: 10.1021/ja02268a002

(38) Freundlich, H. *J. Phys. Electrochem.* **1906,** *57*, 385.

(39) Hameed, B. H. *J. Hazard. Mater.* **2008,** *154*, 204. doi: 10.1016/j.jhazmat.2007.10.010

(40) Radovic, L. R.; Moreno-Castilla, C.; Rivera-Utrilla, J. Carbon Materials as Adsorbents in Aqueous Solutions. In *Chemistry and Physics of Carbon*; Radovic, L. R. Ed.; Marcel Dekker: New York, 2001; Vol. 27, pp 227–405.

(41) Ersoz, A.; Denizli, A.; Sener, I.; Atilir, A.; Diltemiz, S.; Say, R. *Sep. Purif. Technol.* **2004,** *38*, 173. doi: 10.1016/j.seppur.2003.11.004

(42) Chandra, V.; Park, J.; Chun, Y.; Lee, J. W.; Hwang, I. C.; Kim, K. S. *ACS Nano* **2010,** *4*, 3979. doi: 10.1021/nn1008897

(43) Coughlin, R. W.; Ezra, F. S. *Environ. Sci. Technol.* **1968,** *2*, 291. doi: 10.1021/es60016a002